Original Article

JCBFM

Journal of Cerebral Blood Flow & Metabolism
2021, Vol. 41(1) 67–81

DOI: 10.1177/0271678X19898148
journals.sagepub.com/home/jcbfm
SAGE

DSC perfusion-based collateral imaging and quantitative T2 mapping to assess regional recruitment of leptomeningeal collaterals and microstructural cortical tissue damage in unilateral steno-occlusive vasculopathy

Alexander Seiler[1,2], Annemarie Brandhofe[1,2], René-Maxime Gracien[1,2], Waltraud Pfeilschifter[1], Elke Hattingen[3], Ralf Deichmann[2], Ulrike Nöth[2] and Marlies Wagner[3]

Abstract

Leptomeningeal collateral supply is considered pivotal in steno-occlusive vasculopathy to prevent chronic microstructural ischaemic tissue damage. The aim of this study was to assess the alleged protective role of leptomeningeal collaterals in patients with unilateral high-grade steno-occlusive vasculopathy using quantitative (q)T2 mapping and perfusion-weighted imaging (PWI)-based collateral abundance. High-resolution qT2 was used to estimate microstructural damage of the segmented normal-appearing cortex. Volumetric abundance of collaterals was assessed based on PWI source data. The ratio relative cerebral blood flow/relative cerebral blood volume (rCBF/rCBV) as a surrogate of relative cerebral perfusion pressure (rCPP) was used to investigate the intravascular hemodynamic competency of pial collateral vessels and the hemodynamic state of brain parenchyma. Within the dependent vascular territory with increased cortical qT2 values ($P = 0.0001$) compared to the contralateral side, parenchymal rCPP was decreased ($P = 0.0001$) and correlated negatively with increase of qT2 ($P < 0.05$). Furthermore, volumetric abundance of adjacent leptomeningeal collaterals was significantly increased ($P < 0.01$) and negatively correlated with changes of parenchymal rCPP ($P = 0.01$). Microstructural cortical damage is closely related to restrictions of antegrade blood flow despite increased pial collateral vessel abundance. Therefore, increased leptomeningeal collateral supply cannot necessarily be regarded as a sign of effective compensation in patients with high-grade steno-occlusive vasculopathy.

Keywords

Chronic cerebral hypoperfusion, collaterals, cortical microstructure, quantitative magnetic resonance imaging, perfusion-weighted imaging

Received 23 July 2019; Revised 7 November 2019; Accepted 4 December 2019

Introduction

Patients with chronic hemodynamic impairment due to high-grade carotid steno-occlusive disease generally are at risk for ischaemic brain tissue damage,[1,2] which may lead to acute or chronic clinical symptoms. Pathophysiologically, especially the latter may be caused by underlying hypoperfusion-related pathological alterations of tissue microstructure, which are not

[1]Department of Neurology, Goethe University Frankfurt, Frankfurt, Germany
[2]Brain Imaging Center, Goethe University Frankfurt, Frankfurt, Germany
[3]Institute of Neuroradiology, Goethe University Frankfurt, Frankfurt, Germany

Corresponding author:
Alexander Seiler, Department of Neurology, Goethe University Frankfurt, Schleusenweg 2-16, 60528 Frankfurt, Germany.
Email: Alexander.Seiler@kgu.de

detectable on conventional magnetic resonance imaging (MRI). Earlier studies focused mainly on pathological changes of the white matter microstructure in subcortical watershed areas which are vulnerable to critical reductions of perfusion pressure.[3–6] Recently, hypoperfusion-related microstructural changes of the cerebral cortex that has a more complex and variable vascular anatomy and a particularly high demand regarding glucose and oxygen supply,[7,8] are increasingly investigated.[9–13] Previous MRI studies have described a regional association between hemodynamic compromise and cortical thinning.[9,11,12] Quantitative magnetic resonance imaging (qMRI) with T2 mapping has been used for estimation of microstructural tissue damage in the cerebral cortex[14,15] as it should be sensitive to pathological processes like gliotic tissue conversion, increase of extra- and intracellular tissue water content, demyelination and axonal damage which cause a prolongation of transverse relaxation time and therefore increasing qT2 values.[15–17] Since measurable increases of qT2 values seem to occur before visually assessable tissue changes on structural MRI,[14] qT2 mapping may be a highly sensitive imaging marker for investigation of hypoperfusion-related microstructural cortical damage.

Collateral blood flow is presumed to be crucial for maintaining tissue integrity in the condition of cerebral hypoperfusion due to steno-occlusive vasculopathy.[1,18] While the periventricular white matter and the basal ganglia – exclusively supplied by perforating end arteries originating from the M1 segment of the middle cerebral artey[19] – are dependent on the antegrade blood flow, the cortical tissue fraction might benefit from the recruitment of collateral vessels in the close-by leptomeningeal compartment. However, it has been demonstrated that recruitment of collateral pathways – especially the pial collateral vessels – seems to be associated with severe hemodynamic failure,[20,21] and therefore, it is questionable whether collateral recruitment in the long term is sufficient to prevent ischaemic tissue damage.[20] The aim of this study was to investigate the association between microstructural changes in normal-appearing cerebral cortex and the degree of hemodynamic impairment in patients with unilateral steno-occlusive vasculopathy of the anterior circulation with particular focus on collateral supply by applying innovative methodological MRI and postprocessing approaches. For this purpose, the degree of leptomeningeal collateralization is volumetrically quantified from T2*-weighted perfusion-weighted imaging (PWI) magnitude data[22] and high-resolution qT2 mapping is used for detection of pathological changes of cortical microstructure. In addition, hemodynamic properties of antegrade flow and pial collateral vessels are investigated to assess the pathophysiological plausibility and validity of these methods to characterize leptomeningeal collateral supply and microstructural tissue damage of the cerebral cortex.

Materials and Methods

Patients

Thirty patients with symptomatic or asymptomatic occlusive disease of the internal carotid artery (ICA) ($n = 22$) or middle cerebral artery (MCA) ($n = 8$) and without evidence of cortical lesions on structural MRI were included. A proportion of these patients has been described earlier.[14] Inclusion criteria were the following: 1) Doppler/ultrasound evidence of a unilateral high-grade ($\geq$70% according to the North American Symptomatic Carotid Endarterectomy Trial (NASCET) criteria) extracranial ICA stenosis or occlusion; or 2) duplex ultrasonography or MR-angiographic evidence (Figure 1(a)) of a $\geq$50% unilateral intracranial ICA or proximal MCA stenosis/occlusion. Patients with relevant bilateral stenoses ($\geq$50% contralateral ICA or MCA stenosis) were excluded. These degrees of stenosis were chosen as inclusion criteria for patients with ICA, respectively, MCA steno-occlusive vasculopathy since they usually can be assumed to cause relevant perfusion abnormalities which stimulate leptomeningeal collateralization and might induce microstructural tissue damage.[14,21,23] Small subcortical embolic or hemodynamic ischaemic lesions were not expected to substantially influence cortical qT2 values and subcortical perfusion measures and were therefore not considered as an exclusion criterion. Patients were considered as asymptomatic if based on the available imaging data, patient records and outpatient reports there were 1) no evidence of ever experienced clinical symptoms attributable to the steno-occlusive vessel pathology and 2) no ischaemic lesions on diffusion-weighted imaging (DWI) and T2-weighted images in the dependent vascular territory compatible with embolic or hemodynamic stroke. Transient ischaemic attacks (TIA) were distinguished from ischaemic strokes based on DWI, which was available for all patients from clinical MRI examinations performed prior to inclusion in our study. According to the established definition of ischaemic stroke, patients were classified as having ischaemic stroke in case of the presence of an ischaemic lesion in the vascular territory depending on the affected vessel, even in case of the absence or the rapid complete resolution of compatible clinical symptoms. Regarding

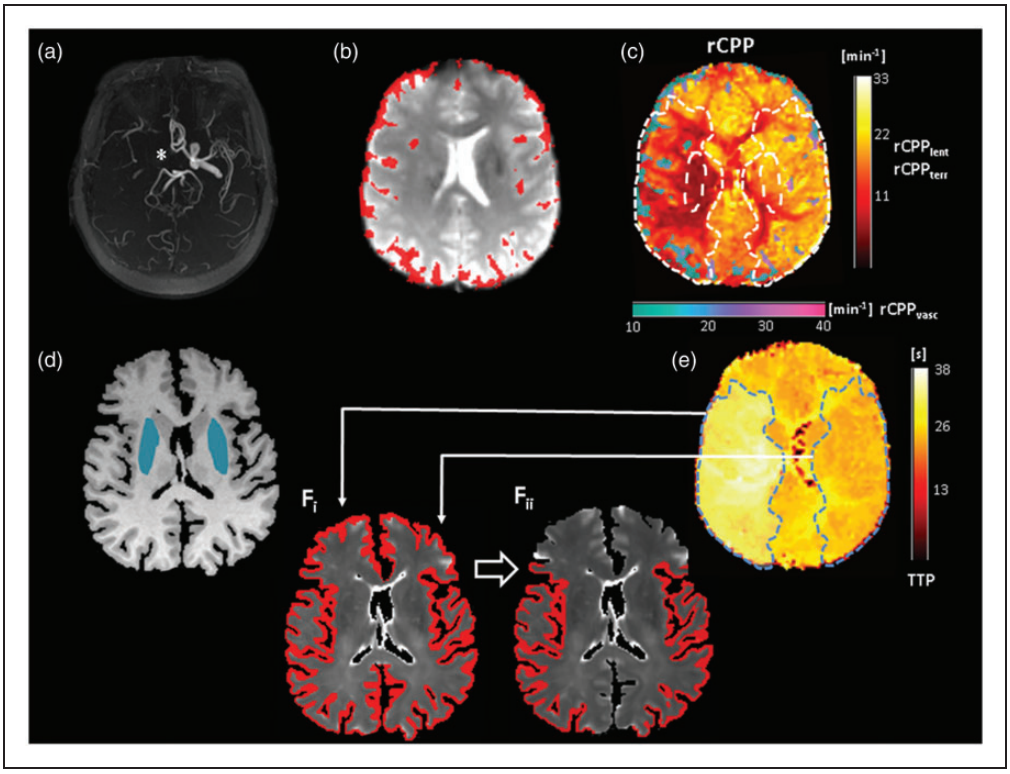

Figure 1. Upper row: Illustration of leptomeningeal collateral vessel map and the rCPP map in a patient with chronic occlusion of the right ICA. (a) ToF-MRA shows a missing flow signal of the right intracranial ICA (*). (b) first volume of the T2*-weighted PWI time series with overlaid pial collateral vessels which were extracted from the PWI data according to a high magnitude of signal variance (upper 50% of the robust range)[22] across time. The resulting binary vessel mask was used to mask maps of the rCPP (calculated as rCBF/rCBV) for tissue and pial collaterals, separately (c). Note the increased abundance of leptomeningeal vessels ipsilateral to the vessel pathology and the distinct drop of rCPP within these collateral vessels and the adjacent hypoperfused tissue (c). (d) T1-weighted image used for tissue segmentation with overlaid masks for the lentiform nucleus derived from MNI standard space. These lentiform nucleus ROIs are also shown as overlays on the rCPP map in (c). (e): TTP map with the region of perfusion delay in the right hemisphere used to generate a volume-based ROI of the dependent vascular territory (light blue area) and the corresponding contralateral region after mirroring to the contralateral side. Both ROIs are also shown as overlays on the rCPP map in (c). (f_i) Quantitative T2 map with overlaid cortex mask obtained from tissue segmentation and further processing. Volume-based ROIs from E were applied to this mask for enabling extraction of qT2 values from cortical tissue in the dependent vascular territory and the corresponding contralateral region (f_{ii}). rCPP: relative cerebral perfusion pressure; TTP: time-to-peak.

symptomatic patients with ischaemic stroke, only subjects with minor stroke were considered for inclusion in the study. In line with a widely accepted definition, a minor stroke was defined as a non-disabling ischaemic stroke with a score of $\leq$3 on the National Institutes of Health Stroke Scale (NIHSS).[24] According to the clinical course before the inclusion in the study, symptomatic patients were classified as recently symptomatic (ischaemic stroke or TIA in the last 30 days before enrollment) or formerly symptomatic (ischaemic stroke or TIA at an earlier time point). The study was approved by the local institutional review board of the Goethe University Frankfurt, Faculty of Medicine (Ethikkomission des Fachbereichs Medizin) and written informed consent was obtained from all subjects before enrollment. The study was conducted in accordance with the Helsinki Declaration (revised version from 1983).

MRI protocol

MRI data were acquired on a 3 T whole-body scanner (Magnetom Trio, Siemens, Erlangen, Germany) using the body coil of the scanner for radiofrequency transmission and an eight-channel phased array head coil for signal reception. The MRI examination included quantitative T2 mapping as well as PWI, conventional T1- and T2-weighted sequences and Time-of-Flight MR-angiography (ToF-MRA).

Anatomic imaging for tissue segmentation was based on a T1-weighted MPRAGE sequence with the following imaging parameters: TR/TE/TI = 1900/

3.04/900 ms, FOV = 256 × 256 × 192 mm^3, whole-brain coverage, isotropic spatial resolution = 1 mm, bandwidth = 170 Hz/pixel, excitation angle = 8°, parallel imaging with reduction factor of 2, duration = 4 min 28 s.

Quantitative T2 mapping was based on a fast spin-echo sequence with an echo-train length of 11 echoes per excitation, an echo spacing of 17.1 ms, and the following imaging parameters: 35 axial slices with 2-mm slice thickness, no interslice gap, TR = 7 s, bandwidth = 100 Hz/pixel, 180° refocusing pulses, matrix size = 192 × 144 (readout × phase encoding), FOV = 240 × 180 mm^2 and in-plane resolution = 1.25 × 1.25 mm^2. For quantitative T2-mapping, five data sets were acquired with different TE values (17, 86, 103, 120, 188 ms), keeping all other acquisition parameters constant. The total duration was 8 min 55 s.

Dynamic susceptibility contrast (DSC) PWI was based on a gradient-echo EPI sequence with the following imaging parameters: TE = 35 ms, TR = 1500 ms, flip angle = 90°, FOV = 230 × 230 mm^2, matrix = 128 × 128, slice thickness = 4 mm with an interslice gap of 1.2 mm, number of slices = 16, in-plane resolution = 1.8 × 1.8 mm^2 and acquisition time = 1 min 15 s. The contrast agent (0.1 mmol/kg of gadobutrol (Gadovist Bayer, Leverkusen, Germany) was injected into an antecubital vein using a power injector at a rate of 5 ml/s followed by a flush with 10 ml of saline. In some patients, PWI was acquired according to a clinical indication on a 3 T whole-body scanner (Magnetom Verio, Siemens) as part of a clinical imaging protocol.

Image postprocessing and analysis

Calculation of qT2 maps. To reduce the influence of subject motion, a target data set was created by calculating the sum-of-squares average of the five T2-weighted data sets acquired at different TE. Subsequently, these source data sets were co-registered to the target. Quantitative T2 maps were obtained pixel-wise from the five co-registered data sets by fitting mono-exponentially the dependence of the T2-weighted signal amplitude on TE.

PWI postprocessing and calculation of collateral vessel maps. PWI raw data were processed off-line at the scanner console using the scanner's software package to generate standard perfusion parameter maps. Maps of the time-to-peak (TTP) were generated by measuring for each voxel the time when the maximum signal decrease after the injection of the contrast bolus occurred. In order to determine the shape of the arterial input function, two experienced neuroradiological readers selected 5–10 voxels of the proximal MCA segment contralateral to the vessel pathology. Maps of relative cerebral blood flow (rCBF) and relative cerebral blood volume (rCBV) were calculated based on the model-independent singular value decomposition method developed by Ostergaard et al.[25,26] For the investigation of the hemodynamic impairment in the dependent vascular territory and the intravascular hemodynamic competency of leptomeningeal collaterals, maps of the rCBF/rCBV ratio were generated voxelwise. Being a measure of local blood flow in relation to vascular tone and vessel density, the ratio CBF/CBV has been validated as a reliable surrogate of local cerebral perfusion pressure (CPP) in positron emission tomography (PET) studies.[27,28] Despite methodological issues regarding the absolute quantification of blood flow with MR-PWI, recent studies suggest that PWI-based rCBF/rCBV can be used[14] to estimate relative CPP (rCPP).

Reliable assessment of pial collateralization in cerebral large-artery steno-occlusive disease requires a technique with adequate sensitivity to detect also late collateral flow in the venous phase to the vascular territory depending on the stenosed/occluded artery. Furthermore, accurate estimation of the individual collateral vessel abundance is essential in order to obtain objective and rater-independent results. Therefore, in this study, DSC-based PWI is used for collateral assessment, thereby exploiting the contrast agent-related signal change over the entire acquisition time as described before.[22] Voxels representing leptomeningeal collateral vessels were extracted from the T2*-weighted PWI source data according to the magnitude of signal variance over time induced by the contrast agent as previously described.[22] In more detail, using a custom-built shell script applying tools from the FMRIB software library (FSL, Version 5.0; https://fsl.fmrib.ox.ac.uk/fsl), voxels of pial collateral vessels were filtered automatically based on their coefficient of variation (CV) regarding the signal-time course in the PWI time series with the following approach: after thorough motion correction, maps depicting the mean signal intensity and the signal standard deviation for each voxel across time were calculated. Afterwards, CV maps were generated by voxel-wise division of the standard deviation by the mean signal intensity. Since larger feeding vessels of the leptomeningeal compartment are characterized by a low mean signal intensity and a large contrast-related signal standard deviation across time, pial collateral vessels were segmented by thresholding the CV maps at the 50th percentile of the robust range for non-zero voxels, thereby keeping only the voxels with the highest signal variance across time. Voxels representing close-by cortical tissue and CSF were corrected for by subtracting the 5% of voxels with the lowest signal intensity at the time point of the maximum contrast-induced signal decrease from

the thresholded CV maps in order to minimize partial volume effects.[22] Collateral vessel abundance as determined with this approach has been demonstrated to reflect the degree of leptomeningeal collateralization, showing a negative association with the ischaemic core volume at admission and a positive association with the amount of salvageable tissue, and predict favourable outcome in ischaemic stroke patients.[22] The resulting collateral vessel maps were binarized (Figure 1(b)) and multiplied with the rCPP maps (Figure 1(c)) to allow for separate analyses of local tissue perfusion pressure in the dependent vascular territory and intravascular perfusion pressure of pial collaterals (Figure 1(c)).

Image co-registration and tissue segmentation. High-resolution qT2 mapping is prone to motion-related artefacts due to the relatively long acquisition times, which are necessary for quantitative mapping. Due to the inherently low anatomic tissue contrast of qT2 maps, motion-induced artefacts might become a relevant problem for multiparametric image analysis in patients with cerebrovascular disease, which involves spatial alignment by co-registration procedures. While the influence of subject motion between different echo times on the image quality can be controlled by performing co-registration of all acquired source data sets to the averaged target data set as explained above, subject motion during acquisition is more likely to compromise data quality. Therefore, all source data sets and the resulting qT2 maps were thoroughly inspected for artefacts by two experienced readers. In the patient cohort, no motion-related artefacts were detected and all calculated qT2 maps could be used for the final analyses. Prior to further postprocessing, all images were skull-stripped. Since quantitative image analysis was performed in the T1-weighted image space, all images and resulting quantitative maps were linearly co-registered to the T1-weighted image. For this purpose, the first three volumes of the PWI time series were averaged to increase anatomic tissue contrast for co-registration and the averaged image was co-registered to the T1-weighted anatomical image. The second T2-weighted image (TE = 86 ms) was also co-registered to the T1-weighted image. The resulting co-registration matrices were used to co-register maps resulting from PWI (including TTP, rCPP and collateral vessel maps) and the qT2 map to the T1-weighted image.

Tissue segmentation of the T1-weighted image (Figure 1(d)) was performed with 'FAST' (FSL),[29] yielding partial volume estimates (PVE) of the cerebral grey matter (GM), white matter (WM) and cerebrospinal fluid (CSF). In order to obtain a segmentation of the cerebral cortex, subcortical GM structures and subcortical lesions misclassified as GM were subtracted from the entire GM estimate by 'filling holes' in the WM mask.[30] Finally, a lower PVE threshold of 0.95 was applied to minimize partial volume effects from the adjacent WM and CSF on the segmented cortex.[31] The resulting cortical template was transformed into a binary mask and applied to the qT2 map to enable extracting qT2 values from cortical tissue (Figure 1(f_i)). This procedure was performed for each patient separately.

Regions-of-interest definition and analysis. Two different sets of regions-of-interest (ROIs) were defined. The first set of ROIs was defined in the lentiform nucleus ipsi- and contralateral to the vascular pathology. Since the lentiform nucleus is exclusively supplied by the perforating lenticulostriate arteries originating from the MCA M1 segment, rCPP extracted from the lentiform nucleus ($rCPP_{lent}$, Figure 1(c)) was expected to reflect the efficacy of antegrade flow to the dependent territory without the influence of leptomeningeal collateralization. ROIs for the lentiform nucleus were generated on a Montreal Neurological Institute (MNI) standard space template and non-linearly co-registered to the respective T1-weighted image of each patient by inverting the warp field obtained from the reciprocal transformation (Figure 1(d)). For the quantitative analysis of imaging parameters in the remaining vascular territory, the second set of ROIs was generated according to a measurable perfusion delay on TTP maps, which allow for definition of the vascular territory depending on the affected artery. This approach was chosen since border zone shift and a variable degree of leptomeningeal collateralization are frequently found in large-artery steno-occlusive disease, resulting in changes of flow territories.[32,33] Thus, a merely anatomic assignment of affected regions may be imprecise. Using hemispheric brain masks created in MNI standard space, voxels in the hemisphere ipsilateral to the vascular pathology with a delayed TTP (mean plus two standard deviations of the contralateral unaffected side) were detected automatically. These areas of TTP-delay were traced manually and extended to the lateral convexity to ensure spatial coverage of the cerebral cortex and the adjacent leptomeningeal compartment (Figure 1(e)). The three-dimensional ROIs were used to estimate the volumetric abundance of pial collateral vessels (Figure 1(b)). Furthermore, the rCPP within leptomeningeal collateral vessels ($rCPP_{vasc}$) and the adjacent tissue belonging to the dependent vascular territory ($rCPP_{terr}$) were extracted from the territory ROIs (Figure 1(c)). All territory ROIs were mirrored to the contralateral side along the median plane for assessment of the respective measures in the corresponding contralateral region (Figure 1(c and e)). The cortical

grey matter mask obtained from tissue segmentation was applied to the qT2 map (Figure 1(f_i)) and masked with the respective territory ROIs on each side to extract qT2 values from cortical tissue (Figure 1(f_{ii})).

Calculation of subcortical ischaemic lesion volume and collection of additional clinical data. Volumes of subcortical lesions resulting from ischaemic stroke in the vascular territory depending on the individually affected artery were delineated manually by two experienced readers in consensus on the second individual T2-weighted image (TE = 86 ms) using the MRIcron software (Chris Rorden, Columbia, SC, USA; www.mricro.com). Along the way, available diffusion-weighted images and patient records concerning symptomatology were taken into consideration to ensure congruence of the delineated lesions with T2-hyperintense lesions resulting from ischaemic stroke caused by the vascular pathology. For assessment of a potential neurological deficit, NIHSS scores were drawn from outpatient reports, respectively, patient records which were available for all included patients within a close time frame to the imaging examination. In addition, information on disease duration regarding the steno-occlusive vasculopathy was collected from all disposable patient records.

For assessment of relative changes in the dependent vascular territory, a hemispheric asymmetry index (AI) was computed for all imaging parameters applying the following formula[34,35]

$$AI = (R_i - R_c)/(R_i + R_c) * 2 * 100\ (\%)$$

Here, R_i and R_c represent the values from the ipsi- and the contralateral regions-of-interest, respectively.

Statistical analysis

The Kolmogorov–Smirnov test showed a deviation from normal distribution for several of the investigated parameters. Therefore, we only applied non-parametric statistical testing. Parameter values between the dependent vascular territory and the corresponding contralateral region were compared with the Wilcoxon-signed rank test. Spearman's rank correlation was applied to test for significant parameter correlations. The Kruskal–Wallis H was used to assess statistically significant differences between groups. Statistical analysis was performed by the means of SPSS 22 (IBM, Armonk, NY, USA). All tests were two-sided and statistical significance was set to $P < 0.05$. Multiple statistical testing was accounted for by performing false discovery rate (FDR) correction for all parameters. Parameter values are given as mean ± standard deviation throughout the subsequent results section unless stated otherwise.

Results

Mean age of the included patients ($n = 30$) was 61.7 ± 14 years, 5 (16.7%) were female. In total, 22 patients (73.3%) had a formerly or recently symptomatic vessel pathology and 8 patients (26.7%) had a completely asymptomatic steno-occlusive vasculopathy. Information on disease duration prior to inclusion in this study could be obtained for 16 patients (53.3%). For the other 14 patients (46.7%), the ischaemic symptoms related to TIA or minor stroke had been the first manifestation of the vascular pathology and thus for these patients no reliable information on disease duration can be provided. For formerly and recently symptomatic patients, median NIHSS at the time of the imaging examination was 1. Mean subcortical ischaemic lesion volume in the dependent vascular territory for patients with formerly or recently sustained ischaemic stroke was 2.43 ± 0.95 cm^3. Mean degree of stenosis was 85.2% ± 7.1% for patients with ICA steno-occlusive disease and 62.5% ± 10.6% for patients with MCA steno-occlusive disease. Demographic and clinical baseline characteristics of all patients are summarized in Table 1.

Cortical qT2 and rCPP in relation to local recruitment of leptomeningeal collaterals

Across the entire cohort ($n = 30$), there was a significant reduction of $rCPP_{lent}$ and $rCPP_{terr}$ ipsilateral to the vascular pathology as compared to the contralateral side (23.75 ± 12.13/min vs. 27.32 ± 13.75/min, $AI = -6.86\% \pm 10.97\%$, $P = 0.0001$ and 20.01 ± 10.4/min vs. 24.3 ± 12.22/min, $AI = -20.2\% \pm 20.15\%$, $P = 0.0001$), while the volumetric abundance of leptomeningeal collaterals was significantly increased (18 ± 13.89 cm^3 vs. 15.3 ± 12.1 cm^3, $AI = 14.97\% \pm 24.39\%$, $P = 0.002$, Figure 2(a)). Within leptomeningeal collateral vessels, a significant decline of $rCPP_{vasc}$ was found (12.61 ± 8.22/min vs. 13.63 ± 8.45/min, $AI = -9.12 \pm 16.83\%$, $P = 0.009$, Figure 2(b)). Concurrently, cortical qT2 within the dependent vascular territory was significantly prolonged compared to the corresponding contralateral area (150.74 ± 36.71 ms vs. 142.6 ± 29.19 ms, $AI = 4.81\% \pm 5.48\%$, $P = 0.0001$, Figure 2(c)).

The relative changes of both $rCPP_{lent}$ and $rCPP_{terr}$ correlated significantly with the relative pial collateral abundance ($r = -0.446$, $P = 0.013$ and $r = -0.462$, $P = 0.01$, Figure 3(a and d)). No significant relationship was found between relative collateral vessel abundance and relative collateral $rCPP_{vasc}$ ($r = -0.09$, $P = 0.638$). However, relative changes of both $rCPP_{lent}$ and $rCPP_{terr}$ showed strong significant correlations with relative changes of $rCPP_{vasc}$ ($r = 0.545$, $P = 0.002$, $r = 0.627$, $P = 0.0001$, Figure 3(b and e)). Neither

Table 1. Demographic and clinical baseline characteristics of all patients including the respective territory region-of-interest volume.

Patient no.	Age (year)	Sex (F/M)	Affected side	Site of stenosis/ occlusion	Degree of stenosis (%)[a]	Clinical course	Clinical manifestation	NIHSS	Subcortical ischaemic lesion volume (cm^3)	Known disease duration (months)	Territory ROI volume (cm^3)
1	67	M	Left	Extracranial ICA	80	Recently symptomatic	Minor stroke	2	1.46	First manifestation[b]	231.4
2	76	M	Right	Extracranial ICA	95	Recently symptomatic	Minor stroke	2	1.6	57	184.9
3	63	M	Left	Extracranial ICA	70	Recently symptomatic	Minor stroke	2	1	First manifestation	141.6
4	74	M	Left	Extracranial ICA	80	Recently symptomatic	Minor stroke	1	3.8	First manifestation	153.7
5	56	M	Right	Extracranial ICA	80	Recently symptomatic	Minor stroke	2	1.75	1.5	102.5
6	74	M	right	Extracranial ICA	80	Recently symptomatic	TIA	0	1.8	29	294.0
7	68	M	Left	Extracranial ICA	80	Recently symptomatic	Minor stroke	1	2.64	4	61.8
8	47	F	Right	Extracranial ICA	80	Recently symptomatic	Minor stroke	0	2.85	First manifestation	206.1
9	82	M	Right	Extracranial ICA	70	Recently symptomatic	Minor stroke	3	3.2	24	133.2
10	79	M	Right	Extracranial ICA	85	Recently symptomatic	Minor stroke	1	1.03	2	199.6
11	43	M	Right	Extracranial ICA	70	Recently symptomatic	Minor stroke	2	1.87	First manifestation	162.9
12	60	M	Left	Extracranial ICA	100	Formerly symptomatic	TIA	0	0	69	144.5
13	82	M	Right	Extracranial ICA	100	Asymptomatic	n.a.	0	0	53	118.7
14	54	M	Right	Extracranial ICA	100	Asymptomatic	n.a.	0	0	42	193.9
15	62	M	Right	Extracranial ICA	100	Asymptomatic	n.a.	0	0	First manifestation	196.8
16	75	F	Right	Extracranial ICA	100	Asymptomatic	n.a.	0	0	31	155.2
17	62	M	Left	Intracranial ICA	75	Asymptomatic	n.a.	0	0	1	173.7
18	49	M	Left	Extracranial ICA	80	Recently symptomatic	Minor stroke	3	1.98	First manifestation	234.0
19	28	M	Right	MCA	55	Formerly symptomatic	Minor stroke	0	3.06	33	186.2
20	83	F	Left	MCA	80	Recently symptomatic	Minor stroke	2	2.14	First manifestation	149.4
21	49	M	Left	MCA	80	Recently symptomatic	Minor stroke	0	3.36	First manifestation	208.4
22	65	M	Right	Extracranial ICA	100	Asymptomatic	n.a.	0	0	60	135.4
23	50	M	Left	MCA	70	Recently symptomatic	Minor stroke/TIA	0	1.7	First manifestation	198.7
24	54	F	Right	MCA	75	Formerly symptomatic	TIA	0	0	19	211.1
25	53	M	Right	Intracranial ICA	100	Recently symptomatic	TIA	0	0	First manifestation	172.8
26	36	M	Right	MCA	50	Recently symptomatic	Minor stroke	0	2.51	First manifestation	86.3
27	66	M	Left	Intracranial ICA	70	Recently symptomatic	Minor stroke	0	4.4	First manifestation	169.9
28	68	M	Right	Intracranial ICA	80	Asymptomatic	n.a.	0	0	4	88.2
29	74	M	Left	MCA	80	Asymptomatic	n.a.	0	0	1	233.5
30	52	F	Right	MCA	70	Recently symptomatic	TIA	0	0	First manifestation	171.0

F: female; M: male; ICA: internal carotid artery; MCA: middle cerebral artery; ROI: region-of-interest; TIA: transitory ischaemic attack; NIHSS: National Institutes of Health Stroke Scale; n.a.: not applicable

[a]Graduation of stenosis was performed based Doppler/ultrasound or conventional digital subtraction angiography (DSA) applying the (modified) NASCET criteria for patients with extracranial ICA stenosis or based on MR-angiography or conventional DSA applying the warfarin aspirin symptomatic intracranial disease (WASID) criteria for intracranial ICA or MCA stenosis.

[b]For patients whose vessel pathology became apparent for the first time due to ischaemic stroke/TIA in the dependent vascular territory no information on disease duration can be provided.

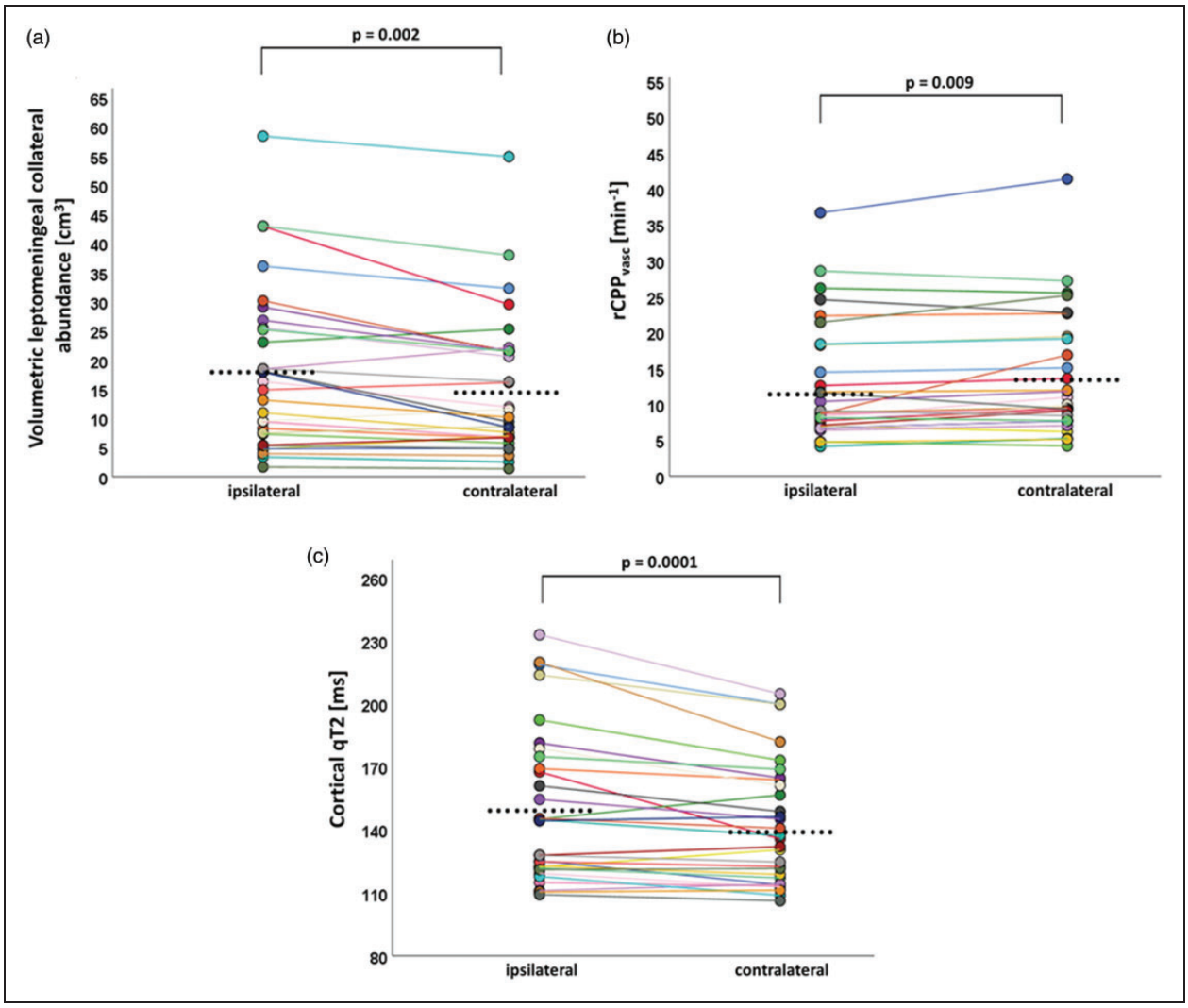

Figure 2. Paired scatter plots illustrating differences regarding the volumetric pial collateral vessel abundance (a), the collateral intravascular perfusion pressure ($rCPP_{vasc}$) (b) and cortical quantitative T2 values (c) between the dependent vascular territory ipsilateral to the vessel pathology and the homologous contralateral region by pair-wise comparison. The dots represent mean parameter values obtained from the respective regions-of-interest. Mean values for each parameter per hemisphere are indicated by the black dots. An individual color is used for each patient consistently throughout all three panels. q: quantitative.

relative collateral vessel abundance nor relative collateral $rCPP_{vasc}$ correlated significantly with relative increase of cortical qT2 ($r = 0.188$, $P = 0.321$ and $r = -0.074$, $P = 0.699$), while relative changes of both $rCPP_{lent}$ and $rCPP_{terr}$ showed a significant negative signed relationship with cortical qT2 increase ($r = -0.423$, $P = 0.02$ and $r = -0.415$, $P = 0.022$, Figure 3(c and f)). Due to a wide scattering of the parameter values (Supplemental Figure), for a better visualization of the significant relationships between the imaging parameters, asymmetry indices of the leptomeningeal collateral abundance, $rCPP_{vasc}$ and cortical qT2 values were subdivided according to four different ranges of the asymmetry indices for $rCPP_{terr}$ and $rCPP_{lent}$ (Figure 3). These four ranges were determined by means of the quartiles of the asymmetry indices: range 1: <25th percentile, range 2: 25th–50th percentile, range 3: 51st–75th percentile and range 4: >75th percentile (Figure 3). Scatterplots illustrating the associations between the different imaging parameters based on the parameter values of all 30 patients are provided in the Supplemental Figure.

Cortical qT2, territorial rCPP and leptomeningeal collateral abundance in relation to subcortical ischaemic lesion volume and disease duration

Territorial rCPP ($rCPP_{terr}$) and relative changes cortical qT2 did not show a significant correlation with the subcortical ischaemic lesion volume ($r = 0.22$, $P = 0.82$

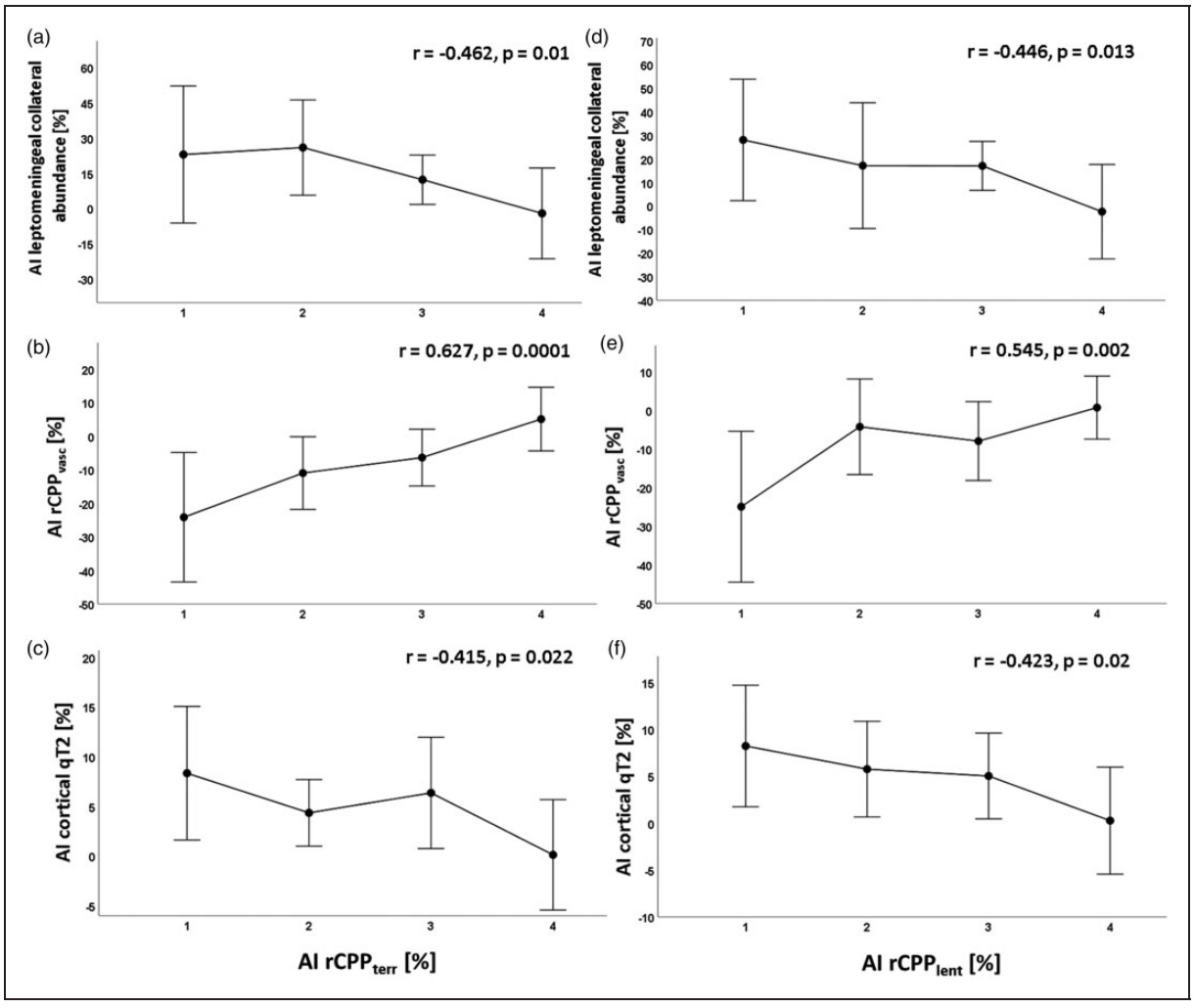

Figure 3. Mean values and standard deviations for relative changes of leptomeningeal collateral abundance, collateral intravascular perfusion pressure ($rCPP_{vasc}$) and cortical qT2 values at four different ranges (1–4) of the hemispheric asymmetry index for $rCPP_{terr}$ (a–c) and $rCPP_{lent}$ (d–f). Ranges for subdivision of $rCPP_{terr}$ and $rCPP_{lent}$ were determined on the basis of the quartiles: 1: <25th percentile; 2: 25th–50th percentile; 3: 51st–75th percentile; 4: >75th percentile. Decreasing $rCPP_{terr}$ and $rCPP_{lent}$ are associated with an increased abundance of leptomeningeal collaterals (a and d), decreasing collateral intravascular perfusion pressure (b and e) and elevated cortical qT2 values (c and f). Correlation coefficients and *P*-values for each pair of parameters are given in the plots. Significant differences ($P < 0.05$) across the four ranges of $rCPP_{terr}$ and $rCPP_{lent}$ were found for all parameters. AI: asymmetry index; q: quantitative; rCPP: relative cerebral perfusion pressure.

and $r = -0.28$, $P = 0.78$). Furthermore, there was no significant correlation between the relative increase of pial collateral vessel abundance and subcortical ischaemic lesion volume ($r = 0.18$, $P = 0.32$). While there were weak and statistically non-significant correlations between $rCPP_{terr}$ and disease duration ($r = -0.108$, $P = 0.69$), respectively between pial collateral vessel abundance and disease duration ($r = 0.062$, $P = 0.82$), there was moderate correlation between relative changes of cortical qT2 and disease duration ($r = 0.453$) which missed statistical significance ($P = 0.077$).

FDR correction was performed for all included parameters and corrected level of significance was $q = 0.026$. Consequently, all significant results maintained statistical significance after correction for multiple comparisons.

Discussion

Using qT2 and PWI-based collateral imaging, this study investigated whether an increased abundance of leptomeningeal collaterals might be protective regarding microstructural cortical damage in unilateral ICA and MCA steno-occlusive disease.

As described above, qT2 was found to be significantly increased in the cortical structures of the dependent territory ipsilateral to the unilateral stenosed artery.

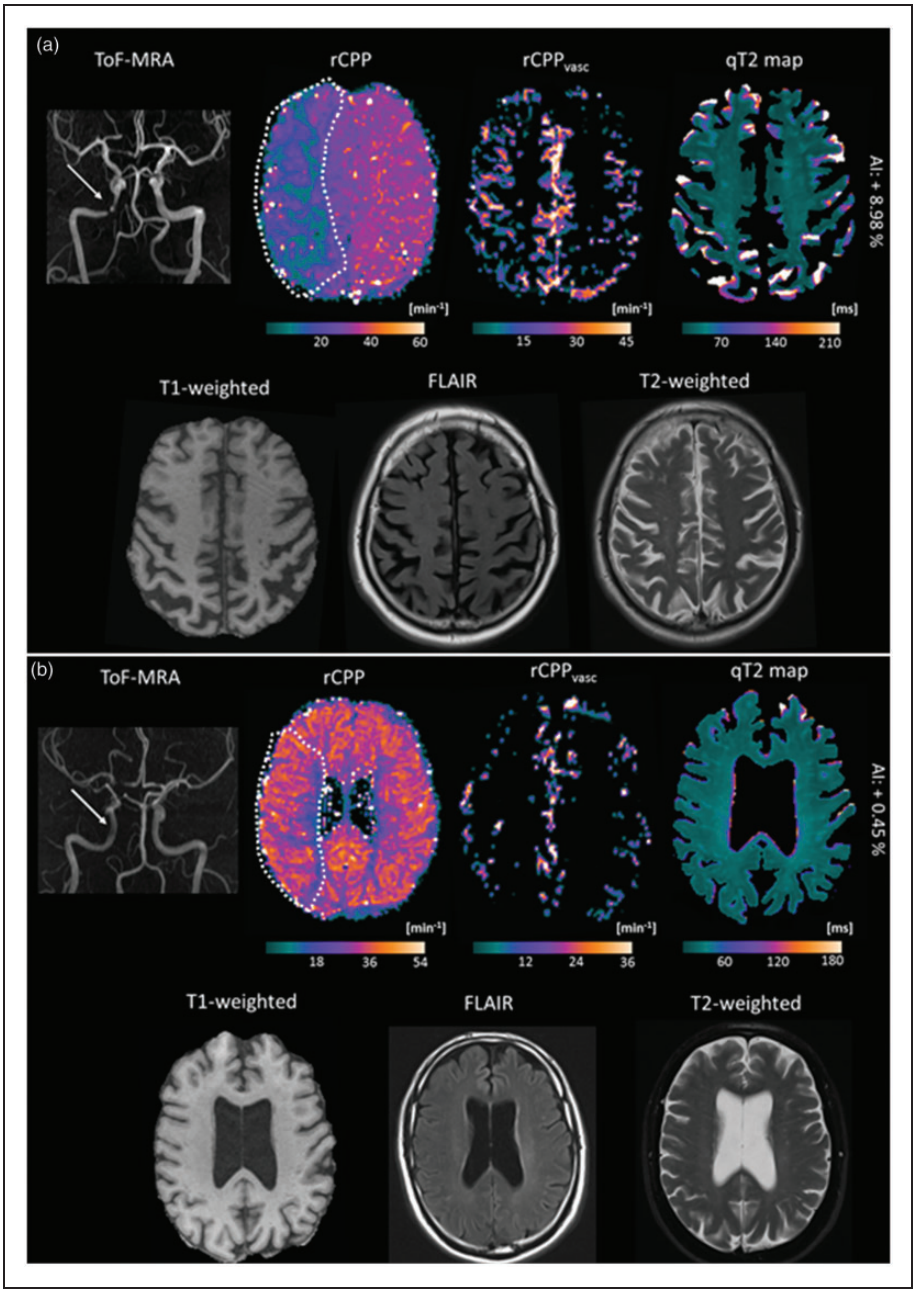

Figure 4. Illustration of imaging parameter results for two representative patients with right-sided high-grade ICA stenosis and different degrees of leptomeningeal collateral recruitment. (a) Patient with a high-grade stenosis (80%) of the right intracranial ICA (white arrow). A pronounced decrease of perfusion pressure (rCPP) can be seen in the dependent vascular territory while the volumetric abundance of leptomeningeal collaterals is considerably increased as depicted by the $rCPP_{vasc}$ map. Higher luminosity on this map reflects higher collateral intravascular perfusion pressure. (b) Patient with a high-grade stenosis (80%) of the right extracranial ICA. The white arrow in the upper left image indicates a slightly reduced flow signal on the MR-angiography in the intracranial segment of the right ICA. A small reduction of tissue perfusion pressure can be seen and the abundance of pial collateral vessels is not increased around the hemisphere ipsilateral to the vessel pathology. While the patient in (a) showed a considerable prolongation of cortical qT2 in the dependent vascular territory as compared to the contralateral side, only a small increase of cortical qT2 in the dependent vascular territory was found for the patient in (b). As relative changes of cortical qT2 ipsilateral to the vessel pathology are difficult to detect visually, they are provided in text form. For better visibility of tissue contrast, brain-extracted qT2 maps are shown after subtraction of CSF in both examples. The broken white line on the tissue rCPP maps represents the margins of the regions-of-interest which were used for the quantitative analyses. ToF-MRA: time-of-flight MR-angiography; rCPP: relative cerebral perfusion pressure; q: quantitative; AI: asymmetry index; FLAIR: fluid-attenuated inversion recovery.

In general, conceivable pathological alterations of cortical microstructure that cause a prolongation of qT2 mainly include extra- and intracellular edema, iron deposition, myelin and axonal damage and gliotic changes.[15–17] Since CBV is usually elevated due to autoregulatory vasodilation in areas with chronically reduced perfusion pressure,[1,36] one might assume that increases of cortical qT2 values are caused primarily by an increase of tissue water content, especially in the extracellular compartment. However, this is unlikely because a reduction of local perfusion pressure can be expected to lower also capillary filtration due to a decreased pressure gradient, resulting in reduced overall tissue water content. A reduction of cortical thickness related to hemodynamic impairment, reflecting reduced neuronal density in chronic cerebral hypoperfusion, has been described in previous studies.[9–12] In the light of these previous results, the prolongation of cortical qT2 probably represents gliotic changes and enlargement of the extracellular compartment leading to relative increases of extracellular tissue water due to neuronal deprivation resulting from critically reduced perfusion and the high vulnerability of cortical neurons ('selective neuronal loss').[8,37] The chronically compromised perfusion in this area is sufficient to avoid immediate cell death due to necrosis but not to prevent slowly-progressing ischaemic tissue damage.[10]

As expected and indicating a hemodynamically relevant stenosis, ipsilateral to the vessel pathology a significant decline of rCPP was found within the ipsilateral lentiform nucleus and the remaining dependent vascular territory as a sign of decreased tissue perfusion pressure. At the same time, the abundance of leptomeningeal collateral vessels was significantly increased based on objective volumetric measurements and a decreasing rCPP in the ipsilateral dependent vascular territory was associated with a larger degree of collateralization (Figure 3(a and d)). Since leptomeningeal collateralization is commonly assumed to be stimulated by metabolic distress of affected tissue resulting from hypoperfusion and relative hypoxia,[38] the decrease of tissue perfusion pressure presumably drives the development and increasing recruitment of pial collaterals. This is in line with the results of a previous study demonstrating an association between a hemodynamic deterioration in the dependent vascular territory and leptomeningeal collateralization.[20] To what extent, however, leptomeningeal collaterals are indeed protective regarding microstructural cortical damage, remains somewhat unclear. In any case, increasing abundance of leptomeningeal collateral seems not to be able to compensate completely for decreased antegrade flow. On the one hand, there was a significant increase of cortical qT2 values in the dependent vascular territory compared to the contralateral side indicating microstructural damage of affected ipsilateral cerebral cortex that was significantly negatively correlated with relative changes of rCPP in the basal ganglia and the remaining dependent vascular territory (Figure 3(c and f)). On the other hand, increasing abundance of leptomeningeal collaterals was associated with decreasing rCPP – as suspected earlier,[20] and interestingly, neither collateral abundance nor rCPP within collaterals showed an association with microstructural cortical damage (qT2). Furthermore, increasing pial collateral abundance was associated with further decline of rCPP within the dependent vascular territory (Figure 3(a)). One might therefore assume that leptomeningeal collateral activation in high-grade steno-occlusive disease is sufficient to maintain a low level of supply to the cortex avoiding acute ischaemic damage but is not sufficient to prevent chronic hypoxic microstructural damage of the cortex. The latter therefore seems to be primarily related to the compromise of proximal antegrade flow.

Thus, the degree of leptomeningeal collateral supply in some respects reflects disease severity in steno-occlusive vasculopathy[39] without being able to sufficiently meet metabolic needs of affected downstream tissue and preserve normal tissue integrity on the microstructural level, as speculated earlier.[20] The significant reduction of intravascular perfusion pressure ($rCPP_{vasc}$) of pial collaterals raises questions regarding the structural and functional properties of these vessels. A network of leptomeningeal collaterals seems to represent a low-pressure system in which the vascular tone is adjusted to ensure the largest possible quantity of blood flow to the affected territory, which however is not sufficient to prevent chronic ischaemic damage and maintain structural cortical integrity. Supporting this assumption, previous studies showed reduced cerebrovascular reactivity associated with the presence of leptomeningeal collaterals in patients with carotid steno-occlusive disease.[40–42] Collateral and parenchymal hemodynamics seem to be intimately linked (Figure 3(b and e)). Therefore, recruitment of leptomeningeal collaterals in patients with chronic steno-occlusive vasculopathy of brain-supplying arteries should make aware of severe hemodynamic impairment potentially compromising integrity of the dependent cortical structures in the longer term. The lack of a significant relationship between the relative reduction of $rCPP_{terr}$ and the volume of subcortical ischaemic lesions suggests that these lesions may be largely embolic and therefore not directly connected to the severity of perfusion impairment. In addition, increases of cortical qT2 values are related to decreases in territorial perfusion pressure (Figure 3(c)) and thus indicate a relative inadequacy of collateral supply, while they are independent from the presence of

subcortical ischaemic lesions. The moderate correlation between the prolongation of cortical qT2 and disease duration ($P = 0.077$) would be plausible from the pathophysiological point of view, as increases of cortical qT2 values seem to reflect pathological tissue alterations resulting from chronically compromised perfusion. However, the information on disease duration still carries considerable uncertainty since vessel pathologies might have existed for several years before they were discovered.

Substantial clinical implications can be drawn from the current study. Firstly, the presence of collaterals in steno-occlusive vasculopathy does not necessarily indicate a sufficiently compensated hemodynamic situation of the affected vascular territory. Collateral vessels should not be disqualified as mere casual bystanders since the hemodynamic situation might be even worse without collateral recruitment and since collateral vessels can be useful in individual cases when relationships between symptomatology and stroke risk together with other clinical factors are considered. This is not possible here due to the sample size and the cross-sectional character of our study. However, rather than indicating an effective compensation and thus protection from ischaemic tissue damage in each individual case, increasing collateral supply may also reflect relevant hemodynamic impairment which induces pathological, most likely chronic ischaemic changes of the cortical microstructure (Figure 4). In line with the presumptions drawn from previous studies the results of this study suggest that the presence of collaterals should at least make aware of a substantially compromised hemodynamic situation with the potential of further deterioration in a state of chronic circulatory deficiency. Secondly, microstructural tissue integrity of the cerebral cortex largely depends on the sufficiency of the antegrade flow to the dependent vascular territory. Thus, with regard to the potential clinical implications of cortical tissue damage, therapeutical options to restore antegrade flow may also be beneficial in patients with distinctive leptomeningeal collateral supply. In contrast to acute ischaemic stroke, where leptomeningeal collaterals are key protective as the main determinant of the progression rate of the ischaemic process and independent predictor of recanalization success, final infarct volume and favorable clinical outcome,[43–47] the ultimate significance of pial collateral recruitment in chronic steno-occlusive vasculopathy is more difficult to define. Presumably, its assessment requires the careful consideration of the clinical course in the individual case. Finally, this study adds to a growing body of evidence concerning the chronic penumbra-like state of the cerebral cortex in chronic cerebral hypoperfusion and its vulnerability on the microstructural level. Further research is necessary to eludicate the role of cortical microstructural changes in the development of chronic clinical symptoms like vascular cognitive impairment.

Limitations

This study has several limitations. It should be noted that in this study mono-exponential fitting was used for qT2 mapping. Yet, due to the co-existence of different water compartments in brain tissue and partial-voluming effects, T2 relaxation shows rather a multi-exponential behavior.[48,49] In fact, multi-exponential fitting would allow for separating different cerebral water compartments and for determining the different water fractions, thus yielding more accurate information about the underlying microstructural tissue composition.[50,51] However, reliable multi-exponential fitting requires a dense sampling of the signal decay curve and thus a comparatively large number of data points (i.e. different echo times)[48,49,52,53], yielding scanning durations which may be problematic in clinical studies. Although the T2 value obtained from mono-exponential fitting rather represents an 'effective' T2 which does not accurately reflect the multi-exponential nature of transverse relaxation,[50] it still permits the reproducible differentiation of pathological from normal tissue upon comparison between patients and healthy control subjects or via between-hemisphere comparisons of the same tissue fraction,[50] as performed in this study. While in several clinical studies two-point methods have been successfully used, in this study five echo times were chosen for mono-exponential fitting, yielding reasonable accuracy for detecting pathological changes of tissue microstructure in a clinical environment. Another limitation is the rather small patient collective and its heterogeneity regarding the site of vessel stenosis/occlusion, the degree of stenosis and the clinical course of the vascular pathology. Given the novelty of the methodological approaches employed in this study, a patient collective with higher degrees of stenosis which is more homogeneous in terms of the location of the vessel pathology might allow for obtaining more generalizable results concerning the imaging parameters and their associations. Furthermore, although changes of qT2 in normal-appearing cortical tissue regardless of the clinical course were found, an interaction between cortical microstructure and certain hemodynamic measurements, which may be different between symptomatic and asymptomatic patients, cannot be completely excluded. In addition, this study was not designed and not powered to comment on the impact of steno-occlusive disease duration and disease progression on the formation of pial collateral vessels and the severity of assumed cortical damage. To address this important

question, a longitudinal design with close-meshed clinical and imaging follow-up examinations would be required. The same holds true for the assessment of potential (partial) reversibility of cortical qT2 prolongation after revascularization. Although this seems to be unlikely, this scenario cannot be entirely excluded since the ultimate mechanisms causing the qT2 prolongation are not fully understood. Even though we found widespread territorial increases of cortical qT2 values and a significant negative relationship with reduction of tissue perfusion pressure in the affected vascular territory, we cannot completely exclude an additional influence of potentially small embolic lesions on cortical T2 values. Finally, it was not possible to relate changes of cortical microstructure to clinical findings like cognitive performance, as clinical features were not systematically evaluated in this study.

Conclusions

In conclusion, recruitment of leptomeningeal collaterals in ICA and MCA steno-occlusive vasculopathy seems not sufficient to compensate completely for impaired antegrade flow regarding chronic ischaemic microstructural cortical tissue damage. Rather than providing full protection and maintaining normal tissue integrity, pial collateral vessels reflect severe hemodynamic impairment of the primary cerebral circulation. Yielding pathophysiologically plausible associations with the severity of hypoperfusion which are in line with the results of previous studies[20,21] and providing an objective and observer-independent measure of leptomeningeal collateral supply,[22] collateral imaging as performed in this study allows for investigating characteristics of pial collateralization. Since the methodological approach presented in this study in based on the calculation of an intraindividual hemispheric asymmetry index of leptomeningeal collateral supply, it can be applied both in patients with acute vessel occlusion[22] and in patients with chronic steno-occlusive vasculopathy, yielding comparably meaningful results. Further evaluation of the relationship between collateral supply and microstructural tissue integrity in a larger patient collective with assessment of additional clinical variables and use of a longitudinal design would be of interest.

Funding

The author(s) received no financial support for the research, authorship, and/or publication of this article.

Declaration of conflicting interests

The author(s) declared no potential conflicts of interest with respect to the research, authorship, and/or publication of this article.

Authors' Contributions

Alexander Seiler – Conceptualization of the study, literature research, development of the method for collateral imaging, MRI image analysis, statistical analysis, writing. Annemarie Brandhofe – Conceptualization of the study, literature research, data interpretation, writing. René-Maxime Gracien – Conceptualization of the study, data interpretation, technical advice regarding data analysis, critical review of the manuscript. Waltraud Pfeilschifter – Collection and interpretation of clinical data, data interpretation, critical review of the manuscript. Elke Hattingen – Statistical analysis, data interpretation, critical review of the manuscript. Ralf Deichmann – Development of the quantitative MRI technique and the motion correction algorithm, critical review of the manuscript. Ulrike Nöth – Development of the quantitative MRI technique and the motion correction algorithm, critical review of the manuscript. Marlies Wagner – Conceptualization of the study, literature research, MRI image analysis, statistical analysis, writing.

Supplemental material

Supplemental material for this article is available online.

References

1. Powers WJ. Cerebral hemodynamics in ischemic cerebrovascular disease. *Ann Neurol* 1991; 29: 231–240.
2. Klijn CJ and Kappelle LJ. Haemodynamic stroke: clinical features, prognosis, and management. *Lancet Neurol* 2010; 9: 1008–1017.
3. Baradaran H, Mtui EE, Richardson JE, et al. White matter diffusion abnormalities in carotid artery disease: a systematic review and meta-analysis. *J Neuroimaging* 2016; 26: 481–488.
4. Soinne L, Helenius J, Saimanen E, et al. Brain diffusion changes in carotid occlusive disease treated with endarterectomy. *Neurology* 2003; 61: 1061–1065.
5. Shiraishi A, Hasegawa Y, Okada S, et al. Highly diffusion-sensitized tensor imaging of unilateral cerebral arterial occlusive disease. *AJNR Am J Neuroradiol* 2005; 26: 1498–1504.
6. Meng X, Jun C, Wang Q, et al. High b-value diffusion tensor imaging of the remote white matter and white matter of obstructive unilateral cerebral arterial regions. *Clin Radiol* 2013; 68: 815–822.
7. Kirkness CJ. Cerebral blood flow monitoring in clinical practice. *AACN Clin Issues*. 2005; 16: 476–487.
8. Yamauchi H, Nishii R, Higashi T, et al. Silent cortical neuronal damage in atherosclerotic disease of the major cerebral arteries. *J Cereb Blood Flow Metab* 2011; 31: 953–961.

9. Fierstra J, Poublanc J, Han JS, et al. Steal physiology is spatially associated with cortical thinning. *J Neurol Neurosurg Psychiatry* 2010; 81: 290–293.
10. Fierstra J, Maclean DB, Fisher JA, et al. Surgical revascularization reverses cerebral cortical thinning in patients with severe cerebrovascular steno-occlusive disease. *Stroke* 2011; 42: 1631–1637.
11. Marshall RS, Asllani I, Pavol MA, et al. Altered cerebral hemodynamics and cortical thinning in asymptomatic carotid artery stenosis. *PLoS One* 2017; 12: e0189727.
12. Lee JJ, Shimony JS, Jafri H, et al. Hemodynamic impairment measured by positron-emission tomography is regionally associated with decreased cortical thickness in Moyamoya phenomenon. *AJNR Am J Neuroradiol* 2018; 39: 2037–2044.
13. Asllani I, Slattery P, Fafard A, et al. Measurement of cortical thickness asymmetry in carotid occlusive disease. *Neuroimage Clin* 2016; 12: 640–644.
14. Seiler A, Deichmann R, Noth U, et al. Extent of microstructural tissue damage correlates with hemodynamic failure in high-grade carotid occlusive disease: an MRI study using quantitative T2 and DSC perfusion. *AJNR Am J Neuroradiol* 2018; 39: 1273–1279.
15. Wagner M, Helfrich M, Volz S, et al. Quantitative T2, T2*, and T2' MR imaging in patients with ischemic leukoaraiosis might detect microstructural changes and cortical hypoxia. *Neuroradiology*. 2015; 57: 1023–1030.
16. Fukunaga M, Li TQ, van Gelderen P, et al. Layer-specific variation of iron content in cerebral cortex as a source of MRI contrast. *Proc Natl Acad Sci U S A*. 2010; 107: 3834–3839.
17. Glasser MF, Goyal MS, Preuss TM, et al. Trends and properties of human cerebral cortex: correlations with cortical myelin content. *Neuroimage* 2014; 93: 165–175.
18. Liebeskind DS. Collateral circulation. *Stroke* 2003; 34: 2279–2284.
19. Tatu L, Moulin T, Bogousslavsky J, et al. Arterial territories of the human brain: cerebral hemispheres. *Neurology* 1998; 50: 1699–1708.
20. Hartkamp NS, Petersen ET, Chappell MA, et al. Relationship between haemodynamic impairment and collateral blood flow in carotid artery disease. *J Cereb Blood Flow Metab* 2018; 38: 2021–2032.
21. Liu S, Luo Y, Wang C, et al. Combination of Plaque Characteristics, Pial Collaterals, and Hypertension Contributes to Misery Perfusion in Patients With Symptomatic Middle Cerebral Artery Stenosis. *J Magn Reson Imaging* 2019; 2020; 51: 195–204.
22. Seiler A, Lauer A, Deichmann R, et al. Signal variance-based collateral index in DSC perfusion: A novel method to assess leptomeningeal collateralization in acute ischaemic stroke. *J Cereb Blood Flow Metab*, Epub ahead of print 13 February 2019. DOI: 10.1177/0271678X19831024.
23. Schroder J, Heinze M, Gunther M, et al. Dynamics of brain perfusion and cognitive performance in revascularization of carotid artery stenosis. *Neuroimage Clin* 2019; 22: 101779.
24. Fischer U, Baumgartner A, Arnold M, et al. What is a minor stroke? *Stroke* 2010; 41: 661–666.
25. Ostergaard L, Weisskoff RM, Chesler DA, et al. High resolution measurement of cerebral blood flow using intravascular tracer bolus passages. Part I: mathematical approach and statistical analysis. *Magn Reson Med* 1996; 36: 715–725.
26. Ostergaard L, Sorensen AG, Kwong KK, et al. High resolution measurement of cerebral blood flow using intravascular tracer bolus passages. Part II: experimental comparison and preliminary results. *Magn Reson Med* 1996; 36: 726–736.
27. Sette G, Baron JC, Mazoyer B, et al. Local brain haemodynamics and oxygen metabolism in cerebrovascular disease. Positron emission tomography. *Brain* 1989; 112: 931–951.
28. Schumann P, Touzani O, Young AR, et al. Evaluation of the ratio of cerebral blood flow to cerebral blood volume as an index of local cerebral perfusion pressure. *Brain* 1998; 121 1369–1379.
29. Zhang Y, Brady M and Smith S. Segmentation of brain MR images through a hidden Markov random field model and the expectation-maximization algorithm. *IEEE Trans Med Imaging* 2001; 20: 45–57.
30. Gracien RM, Reitz SC, Hof SM, et al. Changes and variability of proton density and T1 relaxation times in early multiple sclerosis: MRI markers of neuronal damage in the cerebral cortex. *Eur Radiol* 2016; 26: 2578–2586.
31. Volz S, Noth U, Jurcoane A, et al. Quantitative proton density mapping: correcting the receiver sensitivity bias via pseudo proton densities. *Neuroimage* 2012; 63: 540–552.
32. Chen YF, Tang SC, Wu WC, et al. Alterations of cerebral perfusion in asymptomatic internal carotid artery steno-occlusive disease. *Sci Rep* 2017; 7: 1841.
33. van Laar PJ, Hendrikse J, Klijn CJ, et al. Symptomatic carotid artery occlusion: flow territories of major brain-feeding arteries. *Radiology* 2007; 242: 526–534.
34. Powers WJ, Press GA, Grubb RL Jr., et al. The effect of hemodynamically significant carotid artery disease on the hemodynamic status of the cerebral circulation. *Ann Intern Med* 1987; 106: 27–34.
35. Kado H, Kimura H, Tsuchida T, et al. Abnormal magnetization transfer ratios in normal-appearing white matter on conventional MR images of patients with occlusive cerebrovascular disease. *AJNR Am J Neuroradiol* 2001; 22: 922–927.
36. Derdeyn CP, Videen TO, Yundt KD, et al. Variability of cerebral blood volume and oxygen extraction: stages of cerebral haemodynamic impairment revisited. *Brain* 2002; 125: 595–607.
37. Baron JC, Yamauchi H, Fujioka M, et al. Selective neuronal loss in ischemic stroke and cerebrovascular disease. *J Cereb Blood Flow Metab* 2014; 34: 2–18.
38. Lehoux S and Levy BI. Collateral artery growth: making the most of what you have. *Circ Res* 2006; 99: 567–569.
39. Strother MK, Anderson MD, Singer RJ, et al. Cerebrovascular collaterals correlate with disease severity in adult North American patients with Moyamoya disease. *AJNR Am J Neuroradiol* 2014; 35: 1318–1324.

40. Muller M and Schimrigk K. Vasomotor reactivity and pattern of collateral blood flow in severe occlusive carotid artery disease. *Stroke* 1996; 27: 296–299.
41. Roach BA, Donahue MJ, Davis LT, et al. Interrogating the functional correlates of collateralization in patients with intracranial stenosis using multimodal hemodynamic imaging. *AJNR Am J Neuroradiol* 2016; 37: 1132–1138.
42. Hofmeijer J, Klijn CJ, Kappelle LJ, et al. Collateral circulation via the ophthalmic artery or leptomeningeal vessels is associated with impaired cerebral vasoreactivity in patients with symptomatic carotid artery occlusion. *Cerebrovasc Dis* 2002; 14: 22–26.
43. Copen WA, Rezai Gharai L, Barak ER, et al. Existence of the diffusion-perfusion mismatch within 24 hours after onset of acute stroke: dependence on proximal arterial occlusion. *Radiology* 2009; 250: 878–886.
44. Jovin TG, Liebeskind DS, Gupta R, et al. Imaging-based endovascular therapy for acute ischemic stroke due to proximal intracranial anterior circulation occlusion treated beyond 8 hours from time last seen well: retrospective multicenter analysis of 237 consecutive patients. *Stroke* 2011; 42: 2206–2211.
45. Singer OC, Berkefeld J, Nolte CH, et al. Collateral vessels in proximal middle cerebral artery occlusion: the ENDOSTROKE study. *Radiology* 2015; 274: 851–858.
46. Kucinski T, Koch C, Eckert B, et al. Collateral circulation is an independent radiological predictor of outcome after thrombolysis in acute ischaemic stroke. *Neuroradiology* 2003; 45: 11–18.
47. Bang OY, Saver JL, Buck BH, et al. Impact of collateral flow on tissue fate in acute ischaemic stroke. *J Neurol Neurosurg Psychiatry* 2008; 79: 625–629.
48. Fischer HW, Rinck PA, Van Haverbeke Y, et al. Nuclear relaxation of human brain gray and white matter: analysis of field dependence and implications for MRI. *Magn Reson Med* 1990; 16: 317–334.
49. Laule C, Vavasour IM, Kolind SH, et al. Long T2 water in multiple sclerosis: what else can we learn from multiecho T2 relaxation? *J Neurol* 2007; 254: 1579–1587.
50. Noth U, Shrestha M, Schure JR, et al. Quantitative in vivo T2 mapping using fast spin echo techniques - A linear correction procedure. *Neuroimage*. 2017; 157: 476–485.
51. Woermann FG, Steiner H, Barker GJ, et al. A fast FLAIR dual-echo technique for hippocampal T2 relaxometry: first experiences in patients with temporal lobe epilepsy. *J Magn Reson Imaging* 2001; 13: 547–552.
52. MacKay A, Whittall K, Adler J, et al. In vivo visualization of myelin water in brain by magnetic resonance. *Magn Reson Med* 1994; 31: 673–677.
53. Prasloski T, Madler B, Xiang QS, et al. Applications of stimulated echo correction to multicomponent T2 analysis. *Magn Reson Med*. 2012; 67: 1803–1814.